Hindawi
Journal of Nanomaterials
Volume 2018, Article ID 7083416, 7 pages
https://doi.org/10.1155/2018/7083416

Research Article

Synthesis, Characterization of Nano-β-Tricalcium Phosphate and the Inhibition on Hepatocellular Carcinoma Cells

Langlang Liu, Yanzeng Wu, Chao Xu, Suchun Yu, Xiaopei Wu, and Honglian Dai

State Key Laboratory of Advanced Technology for Materials Synthesis and Processing, Wuhan University of Technology, Wuhan, China

Correspondence should be addressed to Honglian Dai; daihonglian@whut.edu.cn

Received 9 March 2018; Accepted 23 April 2018; Published 6 May 2018

Academic Editor: Victor M. Castaño

It is difficult to synthesize nano-β-tricalcium phosphate (nano-β-TCP) owing to special crystal habit. The aim of this work was to synthesize nano-β-TCP using ethanol-water system and characterize it by X-ray diffraction (XRD), Fourier transform infrared spectroscopy (FTIR), Malvern laser particle size analyzer, and transmission electron microscope (TEM). In addition, the inhibitory effect of nano-β-TCP on human hepatocellular carcinoma (HepG2) cells was also investigated using MTT assay, lactate dehydrogenase (LDH) leakage test, and 4′-6-diamidino-2-phenylindole (DAPI) staining. The results showed that negatively charged rod-like nano-β-TCP with about 55 nm in diameter and 120 nm in length was synthesized, and the average particle size of nano-β-TCP was 72.7 nm. The cell viability revealed that nano-β-TCP caused reduced cell viability of HepG2 cells in a time- and dose-dependent manner. These findings presented here may provide valuable reference data to guide the design of nano-β-TCP-based anticancer drug carrier and therapeutic systems in the future.

1. Introduction

Calcium phosphate is a kind of material which plays an important role in biomedical materials due to its excellent biocompatibility, biological activity, and osteoconductivity [1–5]. Hydroxyapatite (HA) and β-TCP are two of the most widely applied calcium phosphate materials. HA is the main inorganic component of natural bones which has been extensively studied because it can form a mechanically strong bond to natural bone as a ceramic material [6]. However, the biodegradability of HA in the human body is too poor to limit its application [7]. The component of β-TCP is similar to the inorganic component ($Ca_{10}(PO_4)_6(OH)_2$) in the bone matrix [8]. Compared with HA, β-TCP has good biodegradability and higher dissolution rate in the body environment after implantation, which is absorbed and replaced by new bone [9].

In recent years, nanomaterials, due to unique physical and chemical properties, have been widely used in biomedicine, biotechnology, and other fields, including cancer treatment [10], medical imaging [11], and drug carrier [12]. Nano-β-TCP has attracted great attentions in biomedical engineering. For example, high surface energy of nano-β-TCP could be applied to the field of drug delivery, and the use of its small size and large surface area could improve the toughness, biological activity, and biodegradability of material [13–15]. However, as a result of the special crystal habit, it is difficult to synthesize nano-β-TCP. The current literature on preparation of nano-β-TCP has rarely been reported. Liu et al. [16] prepared spherical β-TCP powders with about 100 nm in diameter. Tas et al. [17] synthesized β-TCP with high thermodynamic stability, but particle sizes were submicrometer. Liou and Chen [18] successfully prepared rod-like β-TCP using microwave-assisted coprecipitation method, with about 80–150 nm in diameter and 200–300 nm in length. Nevertheless, on the one hand, the products were large in size and irregular in morphology, which were synthesized by precipitation [16, 19], microwave-assisted coprecipitation, sol-gel method [20], and mechanical synthesis method [21, 22]. On the other hand, the microwave-assisted coprecipitation method has higher requirements for equipment; mechanical synthesis

method spends much time and energy consumption. In addition, grinding media will cause pollution of the product. Room temperature synthesis method [23] has smaller size of the product, but the crystallinity is not good. Therefore, it is of great importance to study the synthesis of nano-β-TCP using a simpler method.

Studies have shown that nano-HA and other nanomaterials have a certain anticancer activity [24–26]. Moreover, the degradation of nano-β-tricalcium phosphate is better than that of HA, but there are few reports on its application in cancer treatment, especially for the treatment of liver cancer. As we know, hepatocellular carcinoma (HepG2) is one of the high incidence of malignant tumors around the world; additionally, HepG2 cell line has been widely used as the human hepatoma model cell line in the development of new antitumor drug carrier and therapeutic systems. Hence, in this study, nano-β-TCP was synthesized from $Ca(NO_3)_2 \bullet 4H_2O$ and $(NH_4)_2HPO_4$ by ethanol-water system (seen in Figure 1), and inhibitory effect of nano-β-TCP was also investigated with the HepG2 cells as the model cell line and human hepatocyte cell (L-02) as the control.

2. Materials and Methods

2.1. Materials. $Ca(NO_3)_2 \bullet 4H_2O$, $(NH_4)_2HPO_4$, anhydrous ethanol, and ammonia solution were purchased from Sinopharm Chemical Reagent Co. (China). Deionized water used in experiment was prepared in our laboratory. HepG2 cells and L-02 cells were provided by China Center for Type Culture Collection. Dulbecco's modified eagle's medium (DMEM), RPMI-1640 medium, phosphate-buffered saline, antibiotic, and antimycotic solution (10,000 U/mL penicillin, 10 mg/mL streptomycin) and trypsin-EDTA were purchased from HyClone (USA). Fetal bovine serum (FBS) and 3-(4,5-dimethyl-2-thiazolyl)-2,5-diphenyl-2H-tetrazolium bromide were provided by Zhejiang Tianhang Biotechnology Co. (China). Lactate dehydrogenase (LDH) detection kit and 4′,6-diamidino-2-phenylindole (DAPI) were purchased from Beyotime Institute of Biotechnology (China).

2.2. Preparation of Nano-β-TCP. Nano-β-TCP used in the experiment was synthesized by ethanol-water system in our laboratory. Briefly, stoichiometric amount of $Ca(NO_3)_2 \bullet 4H_2O$ and $(NH_4)_2HPO_4$ was dissolved in anhydrous ethanol and deionized water, respectively. Then the two solutions were mixed under stirring thoroughly at 40°C and a constant pH value with ammonia solution. After that, the mixed solution was placed in an oven at 30°C. The precipitate was centrifuged, washed with deionized water and anhydrous ethanol several times to remove $NH4^+$ and NO^{3-} ions, and then dried in a vacuum oven at 80°C for 12 h. Finally, the dried powder was calcined at 800°C for 2 h in a muffle furnace and employing a heating rate of 15°C/min. In this paper, the influence of reaction procedures on nano-β-TCP was discussed, and the optimal reaction procedure was selected. Four reaction procedures are given in Table 1.

2.3. Characterization of Nano-β-TCP. The size and zeta potential of nano-β-TCP were analyzed in deionized water or DMEM complete culture medium supplemented with 10% FBS (cDMEM) using the Malvern laser particle size analyzer (ZEN1600, UK). The phase and crystallization of the sample were characterized by X-ray diffraction (D/MAX-RBRU-200B, Japan). The characteristic groups of the sample were studied using Fourier transform infrared spectroscopy (Nicolet 6700, USA). The morphology was observed by field-emission transmission electron microscopy (JEM2100F, Japan).

2.4. Cell Culture. Human hepatocellular carcinoma HepG2 cells and human hepatocyte L-02 cells were cultured in DMEM or RPMI-1640 medium supplemented with 10% FBS and 1% penicillin-streptomycin at 37°C under a humidified atmosphere containing 5% carbon dioxide. Cells were trypsinized with 0.25% trypsin-EDTA and passaged upon attaining 70% confluence in cell culture flasks.

2.5. Cell Viability

2.5.1. MTT Assay. The effects of nano-β-TCP on the viabilities of HepG2 cells and L-02 cells were determined by MTT assay [27, 28]. In brief, the exponentially growing HepG2 cells and L-02 cells were seeded into 96-well plate at a density of 1×10^4cells/well and allowed to attachment for 24 h. Then, the culture medium was replaced by the fresh medium containing different concentrations of nano-β-TCP (0, 50, 100, 200, and 400 μg/mL), respectively. The cells were incubated at 37°C with 5% CO_2 for 48 or 72 h. Afterwards, 20 μL of filtered MTT working solution (5 mg/mL) was added to each well, and the cells were further incubated for 4 h at 37°C to allow the yellow dye to be transformed into blue crystals. Thereafter, the unreacted dye solution was removed and 200 μL of DMSO solution was added. The absorbance value was measured at 490 nm using a full-wavelength microplate reader. Cell viability (%) was calculated according to the following formula: cell viability (%) = $[A_{\text{test}}]/[A_{\text{control}}] \times 100\%$.

2.5.2. Lactate Dehydrogenase (LDH) Release. To evaluate the effect of nano-β-TCP on the membrane integrity of HepG2 cells and L-02 cells, the activity of LDH in extracellular medium was measured [29]. Cells were seeded into 96-well plate at a density of 1×10^4cells/well and allowed to attachment for 24 h. Then, cells were treated by different concentrations of nano-β-TCP (0, 50, 100, 200, and 400 μg/mL) for 48 h. According to the manufacturer's instructions, 120 μL of the supernatant was taken into another 96-well plate, and then 60 μL of LDH assay reaction mixture was added. The mixture was incubated at room temperature for 30 min in the darkness, and the absorbance was measured at 490 nm using a microplate reader.

2.5.3. DAPI Staining. HepG2 cells were treated by different concentrations of nano-β-TCP (0, 50, 100, 200, and 400 μg/mL) for 48 h. At the end of incubation, according to the manufacturer's instructions, DAPI staining solution was added to each well, and the cells were further incubated for 5 min. The effect of nano-β-TCP on cell growth was observed under fluorescence microscope.

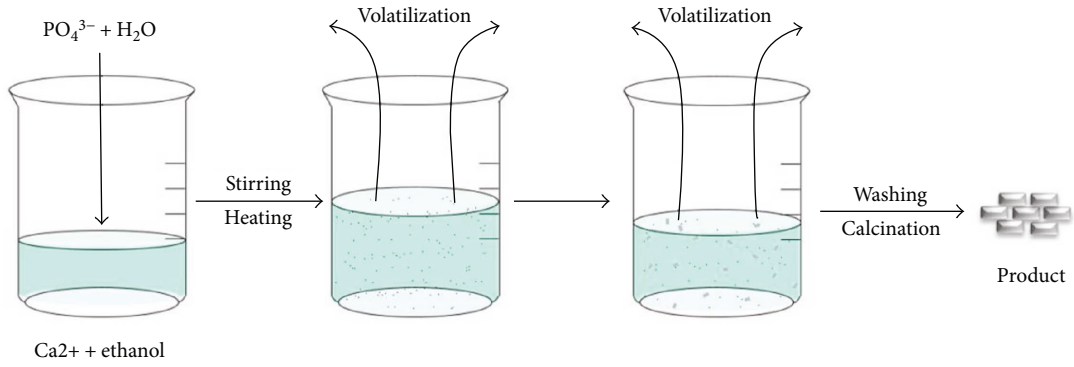

Figure 1: Schematic representation of synthesis of nano-β-TCP by ethanol-water system.

Table 1: Table showing the different reaction procedures between $Ca(NO_3)_2 \bullet 4H_2O$ and $(NH_4)_2HPO_4$.

Procedure	Mixed	Stirring (h)	Dosage of solvent (times) (versus procedure a)
a	Dropwise	4	1
b	Immediately	1	1
c	Dropwise	1	1
d	Dropwise	4	3

2.6. Statistical Analysis. Statistical analysis was performed on Software SPSS17.0. All data were presented as means ± standard deviation (SD). Statistical differences were evaluated using the one-way ANOVA and considered significant when $^*p < 0.05$.

3. Results and Discussion

3.1. Characterization of Nano-β-TCP. The particle size distributions and zeta potential of nano-β-TCP are shown in Figures 2 and 3. The average particle sizes of nano-β-TCP prepared by procedure (a), (b), (c), and (d) were 92.7, 155, 102, and 72.7 nm, respectively. When the dosage of the solvent was increased to three times (versus procedure a), the average particle size of the product decreased from 92.7 to 72.7 nm (Figure 2). By comparison, it can be found that the average particle size of the sample prepared by the experimental process (d) was the smallest. The zeta potential of the nano-β-TCP was negatively charged dispersed in cDMEM, about −8.98 mV (Figure 3); this result agrees well with the finding of Florentina et al. [30].

Calcination temperature and aging time affect the final product in morphology and size. It was observed that both the crystallinity and particle size increased with calcination temperature [20]. The extension of the aging time resulted in the increasement of particle size and agglomeration [31]. Therefore, here, we chose the calcination temperature at 800°C and aging time for 4 h. The driving force for the formation of nano-β-TCP in the ethanol-water system is the difference in Gibbs free energy, which is affected by the reaction temperature and solubility product. Due to the low solubility product of nano-β-TCP, the formation of nano-β-TCP nuclei can be driven by supersaturation at low temperature,

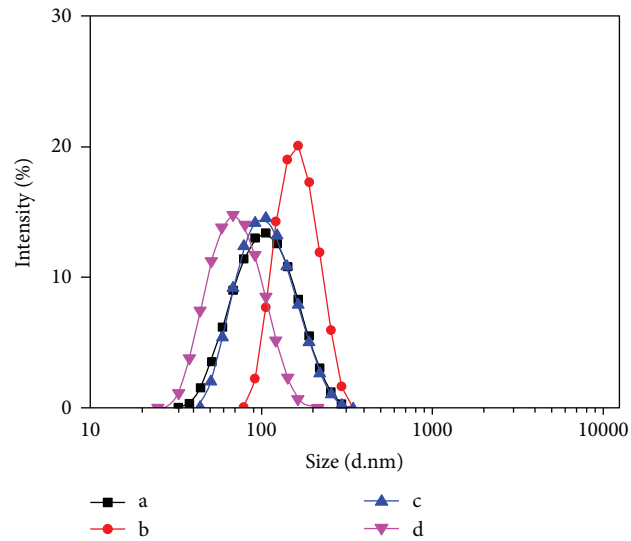

Figure 2: Particle size distributions of nano-β-TCP powders synthesized under different reaction procedures.

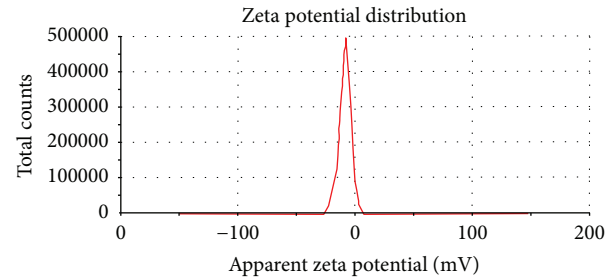

Figure 3: The zeta potential of nano-β-TCP powders synthesized using the experimental procedure (d) dispersed in cDMEM.

and supersaturation helps the nucleation of nano-β-TCP at the beginning of reaction. In the process of reaction and aging, the mixture solution of ethanol and water is more easily evaporated than aqueous solution, resulting in the saturation state of the solution. Therefore, the nucleation and growth process of crystal can be controlled by controlling the rate of evaporation of the solution.

The representative XRD pattern, FTIR, and TEM image of the nano-β-TCP prepared by the experimental process

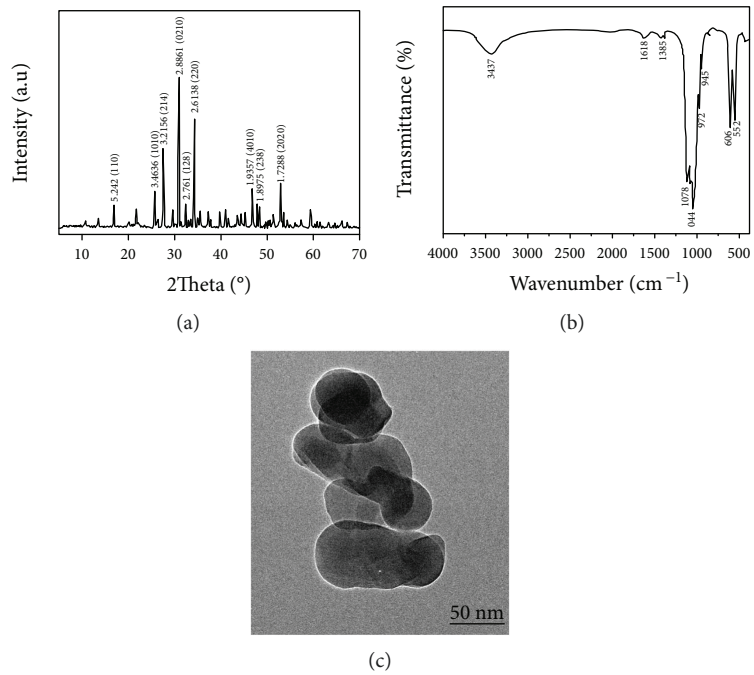

Figure 4: Characterization of nano-β-TCP powders synthesized by the experimental process (d). XRD (a), FTIR (b), and TEM images of nano-β-TCP (c) (scale bar: 50 nm).

(d) are showed in Figure 4. Figure 4(a) exhibits a typical phase composition of nano-β-TCP powder. The diffraction peak of the product was consistent with that of the β-TCP standard card (JCPDS number 09-0169), indicating that the product is high-purity nano-β-TCP with narrow diffraction peak and high strength. Figure 4(b) shows FTIR absorption spectra of nano-β-TCP powder. The bands at 1044 and 1078 cm^{-1} corresponded to the triple degenerate ν_3 antisymmetric stretching vibration of PO_4^{3-}. 972 cm^{-1} band was assigned to ν_1, symmetric stretching vibration of PO_4^{3-}. The bands at 606 and 552 cm^{-1} corresponded to the triple degenerate ν_4 antisymmetric stretching mode. The peaks of the single molecule of adsorbed water were also discerned at 1618 and 3437 cm^{-1}. A weak band near 945 cm^{-1} due to the P-O(H) stretching in HPO_4^{2-} groups was observed. 1385 cm^{-1} band corresponded to the absorption peak of CO_3^{2-}, which may be due to the fact that CO_2 in the air is dissolved in the lattice of nano-β-TCP [32]. A typical TEM image of nano-β-TCP powder obtained by calcination at 800°C, as presented in Figure 4(c), certain agglomeration of nano-β-TCP was observed, due to the large surface area and energy associated to these nanoparticles [33], indicating a short rod shape with a diameter of about 55 nm, 120 nm in length.

3.2. Cell Viability. Many studies have shown that calcium phosphate nanomaterials can obviously inhibit the tumor cell growth [34–36]. The effects of nano-β-TCP on HepG2 cells and L-02 cells were shown in Figures 5 and 6. According to the MTT assay (Figure 5(a)), the cell viability of L-02 cells slightly decreased after nano-β-TCP treatment for 48 h while the metabolic viability of HepG2 cells significantly decreased, indicating that nano-β-TCP has a more significantly inhibitory effect on HepG2 cells. Figure 5(b) shows the cell viability of HepG2 cells after nano-β-TCP treatment with different exposure time and concentrations. When the concentration of nano-β-TCP increased to 400 μg/mL, the cell viability of HepG2 cells decreased to 64.23% and 62.75% at 48 h and 72 h, respectively, indicating that nano-β-TCP caused reduced cell viability of HepG2 cells in a time- and dose-dependent manner. LDH released into the culture medium is also one of the indicators of cytotoxicity, which is used to characterize the integrity of the cell membrane [37]. The release of LDH from HepG2 cells and L-02 cells treated with nano-β-TCP for 48 h was significantly higher than that of the control group (Figure 5(c)). When the concentration of nano-β-TCP was 200 μg/mL, the release of LDH from HepG2 cells and L-02 cells was about 145.39% and 128.09% (versus control group), respectively. However, the concentration continued to increase; LDH slightly decreased but was still higher than the control group, which may be due to the agglomeration and precipitation of nano-β-TCP. Figure 6 shows fluorescence images of HepG2 cells treated with different concentrations of nano-β-TCP for 48 h. HepG2 cells nuclei were stained with DAPI into blue. With the increasement of the concentration of nano-β-TCP, the number of HepG2 cells decreased gradually, and the results were consistent with the MTT assay.

4. Conclusions

In this work, we have successfully prepared negatively charged rod-like nano-β-TCP using ethanol-water system and investigated the inhibitory effect of nano-β-TCP on

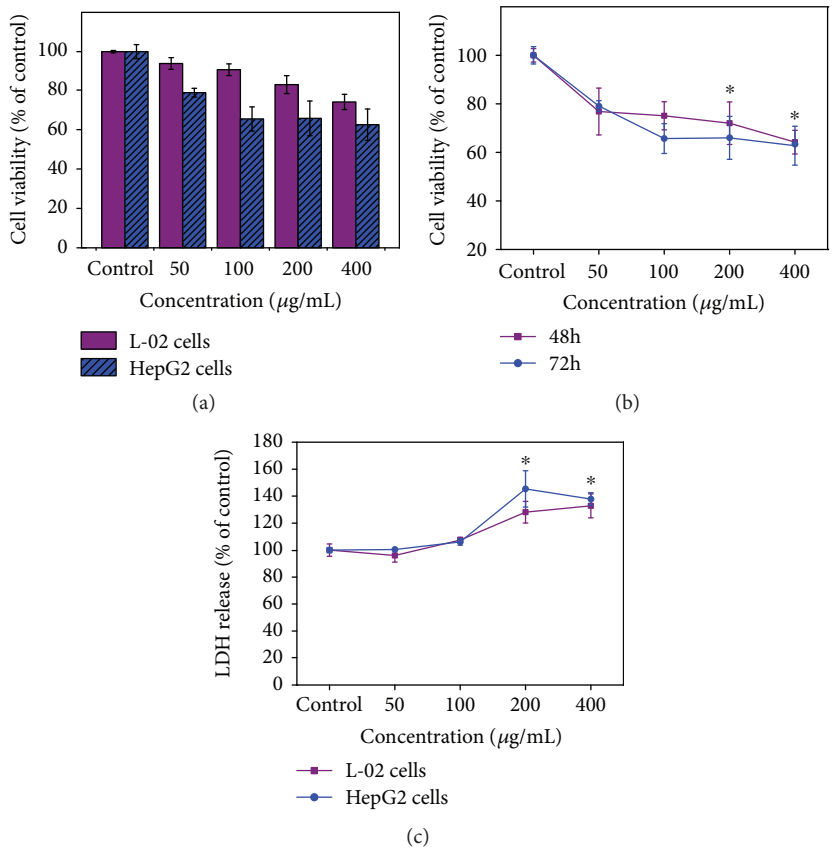

FIGURE 5: (a) Comparison of the cell viabilities of HepG2 cells and L-02 cells treated with different concentrations of nano-β-TCP for 48 h. (b) Dependence of the cell viabilities of HepG2 cells on the incubation time and the concentrations of nano-β-TCP. (c) The activity of extracellular LDH of HepG2 cells and L-02 cells treated with different concentrations of nano-β-TCP for 48 h (versus control group) $^{*}p < 0.05$.

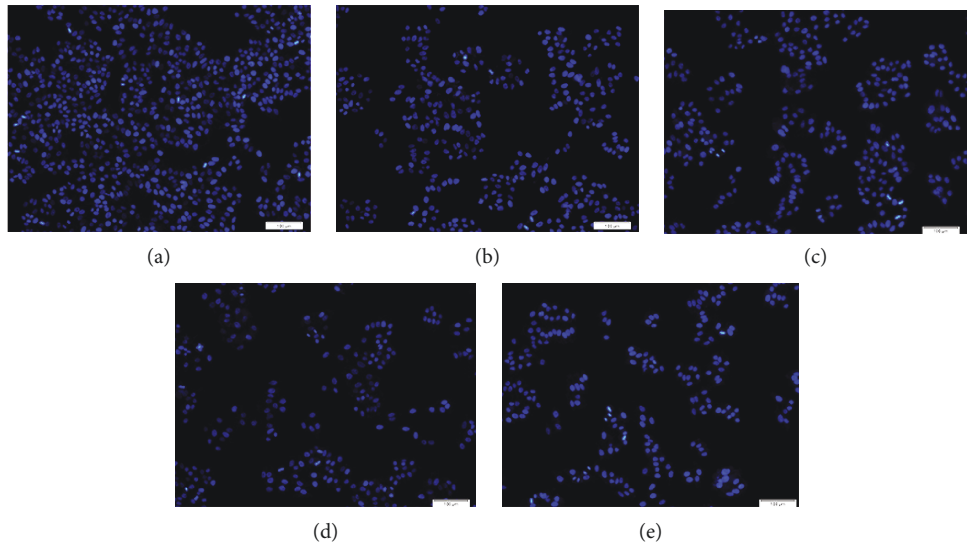

FIGURE 6: Fluorescent micrographs of HepG2 cells after 48 h exposure with nano-β-TCP. (a) Control, (b) 50 μg/mL, (c) 100 μg/mL, (d) 200 μg/mL, and (e) 400 μg/mL. Cell nuclei were stained by DAPI into blue.

HepG2 cells in vitro. Our results showed that the average particle size of nano-β-TCP powder was about 72.7 nm. Nano-β-TCP had a certain inhibitory effect on viability of HepG2 cells in a time- and dose-dependent manner. Additionally, to a certain extent, cell membrane integrity of HepG2 cells was destroyed. These findings presented here

may provide valuable reference data to guide the design of nano-β-TCP-based anticancer drug carrier and therapeutic systems in the future.

Data Availability

The data used to support the findings of this study are included within the article.

Conflicts of Interest

The authors declare no conflict of interest.

Authors' Contributions

Langlang Liu and Yanzeng Wu conceived and designed the experiments. Langlang Liu, Yanzeng Wu, Chao Xu, and Suchun Yu performed the experiments. Langlang Liu and Yanzeng Wu analyzed the data, and Langlang Liu wrote the manuscript. Xiaopei Wu and Honglian Dai contributed to the discussion.

Acknowledgments

This work was supported by the National Key Research and Development Program of China (2016YFC1101605 and 2016YFB1101302), the National Natural Science Foundation of China (51772233 and 81190133), the Key Technology Research and Development Program of Hubei Province (2015BAA085), and the Excellent Dissertation Cultivation Funds of Wuhan University of Technology (2016-YS-011).

References

[1] S. Bose, G. Fielding, S. Tarafder, and A. Bandyopadhyay, "Understanding of dopant-induced osteogenesis and angiogenesis in calcium phosphate ceramics," *Trends in Biotechnology*, vol. 31, no. 10, pp. 594–605, 2013.

[2] J. A. Inzana, D. Olvera, S. M. Fuller et al., "3D printing of composite calcium phosphate and collagen scaffolds for bone regeneration," *Biomaterials*, vol. 35, no. 13, pp. 4026–4034, 2014.

[3] S. Samavedi, A. R. Whittington, and A. S. Goldstein, "Calcium phosphate ceramics in bone tissue engineering: a review of properties and their influence on cell behavior," *Acta Biomaterialia*, vol. 9, no. 9, pp. 8037–8045, 2013.

[4] P. Wang, L. Zhao, J. Liu, M. D. Weir, X. Zhou, and H. H. K. Xu, "Bone tissue engineering via nanostructured calcium phosphate biomaterials and stem cells," *Bone Research*, vol. 2, no. 1, article 14017, 2014.

[5] J. Zhang, W. Liu, V. Schnitzler, F. Tancret, and J. M. Bouler, "Calcium phosphate cements for bone substitution: chemistry, handling and mechanical properties," *Acta Biomaterialia*, vol. 10, no. 3, pp. 1035–1049, 2014.

[6] C. Y. Tan, R. Singh, Y. C. Teh, Y. M. Tan, and B. K. Yap, "The effects of calcium-to-phosphorus ratio on the densification and mechanical properties of hydroxyapatite ceramic," *International Journal of Applied Ceramic Technology*, vol. 12, no. 1, pp. 223–227, 2015.

[7] Y.-H. Yang, C. H. Liu, Y. H. Liang, F. H. Lin, and K. C. W. Wu, "Hollow mesoporous hydroxyapatite nanoparticles (hmHANPs) with enhanced drug loading and pH-responsive release properties for intracellular drug delivery," *Journal of Materials Chemistry B*, vol. 1, no. 19, pp. 2447–2450, 2013.

[8] M. Ito, T. Yamagishi, H. Yagasaki, and A. H. Kafrawy, "*In vitro* properties of a chitosan-bonded bone-filling paste: studies on solubility of calcium phosphate compounds," *Journal of Biomedical Materials Research*, vol. 32, no. 1, pp. 95–98, 1996.

[9] L. Sha, Y. Liu, Q. Zhang, M. Hu, and Y. Jiang, "Microwave-assisted co-precipitation synthesis of high purity β-tricalcium phosphate crystalline powders," *Materials Chemistry and Physics*, vol. 129, no. 3, pp. 1138–1141, 2011.

[10] M. Fiorillo, A. F. Verre, M. Iliut et al., "Graphene oxide selectively targets cancer stem cells, across multiple tumor types: implications for non-toxic cancer treatment, via "differentiation-based nano-therapy"," *Oncotarget*, vol. 6, no. 6, pp. 3553–3562, 2015.

[11] S. Chapman, M. Dobrovolskaia, K. Farahani et al., "Nanoparticles for cancer imaging: the good, the bad, and the promise," *Nano Today*, vol. 8, no. 5, pp. 454–460, 2013.

[12] B. Cao, M. Yang, Y. Zhu, X. Qu, and C. Mao, "Stem cells loaded with nanoparticles as a drug carrier for in vivo breast cancer therapy," *Advanced Materials*, vol. 26, no. 27, pp. 4627–4631, 2014.

[13] A. Ibara, H. Miyaji, B. Fugetsu et al., "Osteoconductivity and biodegradability of collagen scaffold coated with nano-β-TCP and fibroblast growth factor 2," *Journal of Nanomaterials*, vol. 2013, Article ID 639502, 11 pages, 2013.

[14] C. Makarov, I. Berdicevsky, A. Raz-Pasteur, and I. Gotman, "In vitro antimicrobial activity of vancomycin-eluting bioresorbable β-TCP-polylactic acid nanocomposite material for load-bearing bone repair," *Journal of Materials Science: Materials in Medicine*, vol. 24, no. 3, pp. 679–687, 2013.

[15] S. Murakami, H. Miyaji, E. Nishida et al., "Dose effects of beta-tricalcium phosphate nanoparticles on biocompatibility and bone conductive ability of three-dimensional collagen scaffolds," *Dental Materials Journal*, vol. 36, no. 5, pp. 573–583, 2017.

[16] Y. H. Liu, S. M. Zhang, L. Liu et al., "Rapid wet synthesis of nano-sized β-TCP by using dialysis," *Key Engineering Materials*, vol. 330-332, pp. 199–202, 2007.

[17] A. Cüneyt Taş, F. Korkusuz, M. Timuçin, and N. Akkaş, "An investigation of the chemical synthesis and high-temperature sintering behaviour of calcium hydroxyapatite (HA) and tricalcium phosphate (TCP) bioceramics," *Journal of Materials Science: Materials in Medicine*, vol. 8, no. 2, pp. 91–96, 1997.

[18] S. C. Liou and S. Y. Chen, "Transformation mechanism of different chemically precipitated apatitic precursors into β-tricalcium phosphate upon calcination," *Biomaterials*, vol. 23, no. 23, pp. 4541–4547, 2002.

[19] B. Mirhadi, B. Mehdikhani, and N. Askari, "Synthesis of nano-sized β-tricalcium phosphate via wet precipitation," *Processing and Application of Ceramics*, vol. 5, no. 4, pp. 193–198, 2011.

[20] K. P. Sanosh, M. C. Chu, A. Balakrishnan, T. N. Kim, and S. J. Cho, "Sol–gel synthesis of pure nano sized β-tricalcium phosphate crystalline powders," *Current Applied Physics*, vol. 10, no. 1, pp. 68–71, 2010.

[21] D. Choi and P. N. Kumta, "Mechano-chemical synthesis and characterization of nanostructured β-TCP powder," *Materials Science and Engineering: C*, vol. 27, no. 3, pp. 377–381, 2007.

[22] Y. Pan, J. L. Huang, and C. Y. Shao, "Preparation of β-TCP with high thermal stability by solid reaction route," *Journal of Materials Science*, vol. 38, no. 5, pp. 1049–1056, 2003.

[23] J.-S. Bow, S.-C. Liou, and S.-Y. Chen, "Structural characterization of room-temperature synthesized nano-sized β-tricalcium phosphate," *Biomaterials*, vol. 25, no. 16, pp. 3155–3161, 2004.

[24] L. Wang, G. Zhou, H. Liu et al., "Nano-hydroxyapatite particles induce apoptosis on MC3T3-E1 cells and tissue cells in SD rats," *Nanoscale*, vol. 4, no. 9, pp. 2894–2899, 2012.

[25] J. Xu, P. Xu, Z. Li, J. Huang, and Z. Yang, "Oxidative stress and apoptosis induced by hydroxyapatite nanoparticles in C6 cells," *Journal of Biomedical Materials Research Part A*, vol. 100A, no. 3, pp. 738–745, 2012.

[26] Y. Yuan, C. Liu, J. Qian, J. Wang, and Y. Zhang, "Size-mediated cytotoxicity and apoptosis of hydroxyapatite nanoparticles in human hepatoma HepG2 cells," *Biomaterials*, vol. 31, no. 4, pp. 730–740, 2010.

[27] J. Wang, Y. An, F. Li et al., "The effects of pulsed electromagnetic field on the functions of osteoblasts on implant surfaces with different topographies," *Acta Biomaterialia*, vol. 10, no. 2, pp. 975–985, 2014.

[28] H. Xiong, S. du, J. Ni, J. Zhou, and J. Yao, "Mitochondria and nuclei dual-targeted heterogeneous hydroxyapatite nanoparticles for enhancing therapeutic efficacy of doxorubicin," *Biomaterials*, vol. 94, pp. 70–83, 2016.

[29] V. Sharma, D. Anderson, and A. Dhawan, "Zinc oxide nanoparticles induce oxidative DNA damage and ROS-triggered mitochondria mediated apoptosis in human liver cells (HepG2)," *Apoptosis*, vol. 17, no. 8, pp. 852–870, 2012.

[30] F. Grigore, E. Andronescu, S. Gavriliu, M. Lungu, and C. Tardei, "Characterizations of the β-TCP Suspensions," *Revista de Chimie-Bucharest*, vol. 60, pp. 1107–1109, 2015.

[31] A. E. Y. A. Massit, B. C. E. Idrissi, and K. Yamni, "Synthesis and characterization of nano-sized β-tricalcium phosphate: effects of the aging time," *IOSR Journal of Applied Chemistry*, vol. 7, no. 7, pp. 57–61, 2014.

[32] A. H. Rajabi-Zamani, A. Behnamghader, and A. Kazemzadeh, "Synthesis of nanocrystalline carbonated hydroxyapatite powder via nonalkoxide sol–gel method," *Materials Science and Engineering: C*, vol. 28, no. 8, pp. 1326–1329, 2008.

[33] C. L. Martin, D. Bouvard, and G. Delette, "Discrete element simulations of the compaction of aggregated ceramic powders," *Journal of the American Ceramic Society*, vol. 89, no. 11, pp. 3379–3387, 2006.

[34] S.-H. Chu, D.-F. Feng, Y.-B. Ma, and Z.-Q. Li, "Hydroxyapatite nanoparticles inhibit the growth of human glioma cells in vitro and in vivo," *International Journal of Nanomedicine*, vol. 7, pp. 3659–3666, 2012.

[35] Y. Han, S. Li, X. Cao et al., "Different inhibitory effect and mechanism of hydroxyapatite nanoparticles on normal cells and cancer cells *in vitro* and *in vivo*," *Scientific Reports*, vol. 4, no. 1, article 7134, 2014.

[36] F. Qing, Z. Wang, Y. Hong et al., "Selective effects of hydroxyapatite nanoparticles on osteosarcoma cells and osteoblasts," *Journal of Materials Science: Materials in Medicine*, vol. 23, no. 9, pp. 2245–2251, 2012.

[37] S. Gurunathan, J. W. Han, J. H. Park, and J.-H. Kim, "An in vitro evaluation of graphene oxide reduced by *Ganoderma* spp. in human breast cancer cells (MDA-MB-231)," *International Journal of Nanomedicine*, vol. 9, no. 1, pp. 1783–1797, 2014.